

Continuous microfluidic DNA extraction using phase-transfer magnetophoresis

Marc Karle,^{*a} Junichi Miwa,^b Gregor Czilwik,^a Volker Auwärter,^c Günter Roth,^{abd} Roland Zengerle^{abd} and Felix von Stetten^{ab}

Received 18th June 2010, Accepted 9th September 2010

DOI: 10.1039/c0lc00129e

This paper reports a novel microfluidic-chip based platform using “phase-transfer magnetophoresis” enabling continuous biomolecule processing. As an example we demonstrate for the first time continuous DNA extraction from cell lysate on a microfluidic chip. After mixing bacterial *Escherichia coli* culture with superparamagnetic bead suspension, lysis and binding buffers, DNA is released from cells and captured by the beads. These DNA carrying beads are continuously transported across the interfaces between co-flowing laminar streams of sample mixture, washing and elution buffer. Bead actuation is achieved by applying a time-varying magnetic field generated by a rotating permanent magnet. Flagella-like chains of magnetic beads are formed and transported along the microfluidic channels by an interplay of fluid drag and periodic magnetic entrapment. The turnover time for DNA extraction was approximately 2 minutes with a sample flow rate of $0.75 \mu\text{l s}^{-1}$ and an eluate flow rate of $0.35 \mu\text{l s}^{-1}$. DNA recovery was 147% (on average) compared to bead based batch-wise extraction in reference tubes within a dilution series experiment over 7 orders of magnitude. The novel platform is suggested for automation of various magnetic bead based applications that require continuous sample processing, e.g. continuous DNA extraction for flow-through PCR, capture and analysis of cells and continuous immunoassays. Potential applications are seen in the field of biological safety monitoring, bioprocess control, environmental monitoring, or epidemiological studies such as monitoring the load of antibiotic resistant bacteria in waste water from hospitals.

Introduction

Microfluidic platforms¹ are extremely attractive for various bioengineering applications, given their potential of miniaturising, integrating and automating biochemical processes into a small, palm-top-sized chip. Numerous microfluidic technologies for nucleic acid analysis have been developed with the main focus on on-chip PCR.² Recently, the miniaturisation and on-chip integration of labour-intensive sample preparation processes are being featured³ as important steps towards the construction of true micro-total-analysis systems.

Nucleic acid extraction and/or purification is one of the essential steps required in the workflow of genetic analyses. The use of microfluidic technologies leads to substantial reduction of workload and valuable sample or reagent volumes. Therefore various techniques that enable on-chip nucleic acid extraction have been reported.^{4,5} Continuous processing of samples would be highly relevant for many areas such as blood monitoring, process control in pharmaceutical fermentations or the field of security (e.g.

detection of pathogens), but so far devices capable of DNA extraction in such continuous operation modes do not exist.

Among the various nucleic acid extraction methods, we focus on solid phase extraction using magnetic beads. This method is very suitable for implementation in continuous microfluidic processing⁶ because of the mobility of the solid phase and relatively simple equipment required to manoeuvre the beads. The usefulness of magnetic beads in microfluidics has already been shown for several bioassays.^{7–11} For DNA extraction, the use of superparamagnetic beads has been demonstrated on surfaces¹² or in a hydrophobic environment.¹³ Superparamagnetic beads have been used also on a centrifugal microfluidic platform to extract DNA from whole blood¹⁴ in a batch-wise manner.

Free-flow magnetophoresis,¹⁵ which is a technique of separating biomolecules in continuous flow using magnetic beads, seems to be the most attractive for realising continuous on-chip DNA extraction. Its huge potential has been shown through reports on microfluidic cell separation^{16–18} or more recently immunoassays.^{19,20} As mentioned above, so far, a technology for continuous nucleic acid extraction is not available, rendering continuous nucleic acid based total-analysis systems impossible.

In order to enable microfluidic continuous DNA extraction, multiple steps of bead transfer among different extraction buffers have to be integrated on a single chip. Hence, in this work we propose a novel approach which we call “phase transfer magnetophoresis”. In this approach we use free-flow magnetophoresis to transfer magnetic beads across a stable phase interface between streams of different extraction reagents.

^aHSG-IMIT, Wilhelm-Schickard-Strasse 10, 78052 Villingen-Schwenningen, Germany. E-mail: marc.karle@hsg-imit.de; Fax: +49-761-203-7322; Tel: +49-761-203-7329

^bLaboratory for MEMS Applications, Department of Microsystems Engineering - IMTEK, University of Freiburg, Georges-Köhler-Allee 106, 79110 Freiburg, Germany

^cUniversity Medical Centre Freiburg, Institute of Forensic Medicine, Albertstr. 9, 79104 Freiburg, Germany

^dCentre for Biological Signalling Studies (bioss), University of Freiburg, Germany

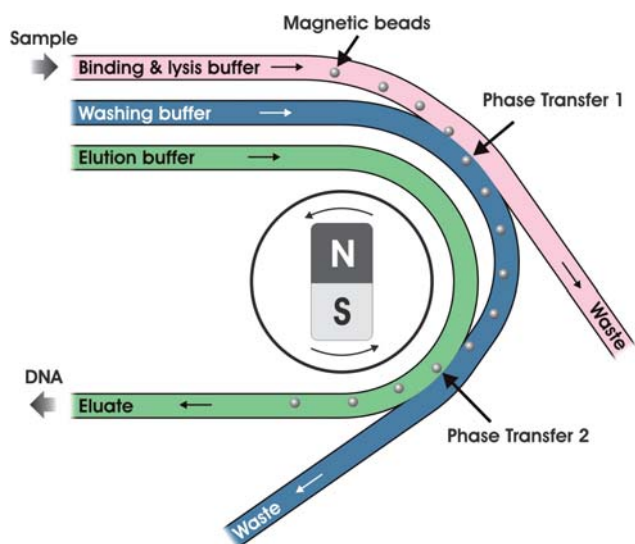


Fig. 1 Schematic view of the microfluidic structure for continuous DNA extraction. The direction of rotation of the central permanent magnet is opposite to the direction of the buffer flow. This platform can also be applied to process other biomolecules if appropriate buffer solutions and magnetic beads are injected into the microchannels.

Using only one rotating permanent magnet we apply a time-varying magnetic field that effectively transfers the superparamagnetic beads among the required buffer solutions in several extraction channels and separation chambers²¹ without immobilizing them to the channel walls. As an example we continuously extracted and purified genomic DNA directly from *Escherichia coli* (*E. coli*) lysate.

System concept and working principle

The continuous extraction of a biomolecule (DNA) from lysed bacterial culture requires three processing steps: binding of the target DNA to superparamagnetic beads, removing of impurities and other undesirable molecules by washing, and elution of the DNA from the beads with elution buffer. On our microfluidic platform these three steps are implemented in a microfluidic structure which is contained in a monolithic and disposable polymer chip.

The required extraction buffers continuously flow through different sections of the chip and DNA-carrying magnetic beads are sequentially transported across the phase interfaces of these different buffer streams. The rotating permanent magnet provides the required magnetic field for bead motion (see Fig. 1). Details of the microfluidic structure and bead actuation are explained in the following two subchapters.

Chip design

The microfluidic chip comprises four different microfluidic elements: inlets, separation chambers, channel junctions and outlets (see Fig. 2). Superparamagnetic beads (Fig. 3b) serve as a mobile solid phase.

Through the three inlets different buffer solutions required for DNA extraction are continuously injected. Three outlets lead to the waste and one outlet guides the eluate containing the purified DNA to subsequent off-chip real-time analysis. The elution channel can selectively be elongated and hence the elution time prolonged by blocking outlet port 4a and retrieving the eluate from outlet port 4b (Fig. 2).

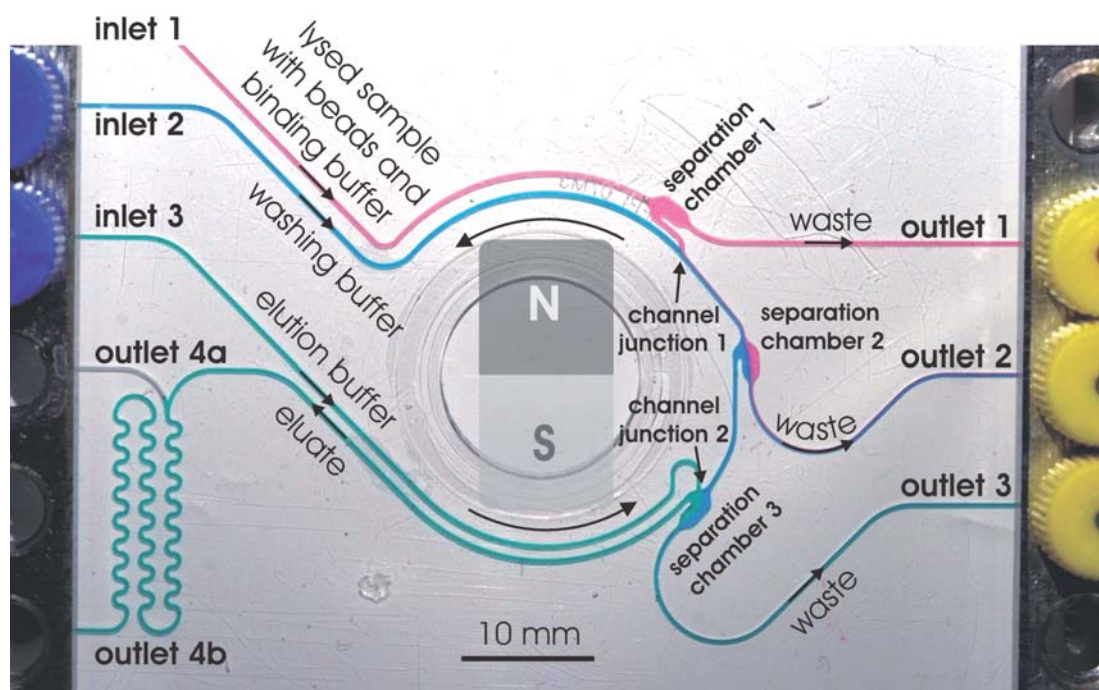


Fig. 2 Photograph of the chip that was used for the extraction experiments. The microchannels have been milled directly into a polycarbonate substrate (blank DVD). To illustrate the extraction process DI water dyed with ink has been injected into the chip (outlet port 4a is blocked and therefore filled with air). The different colours denote the different buffer solutions used for the extraction process. Red: lysis and binding buffer including the cell sample and the magnetic beads, blue: washing solution and green: elution buffer.

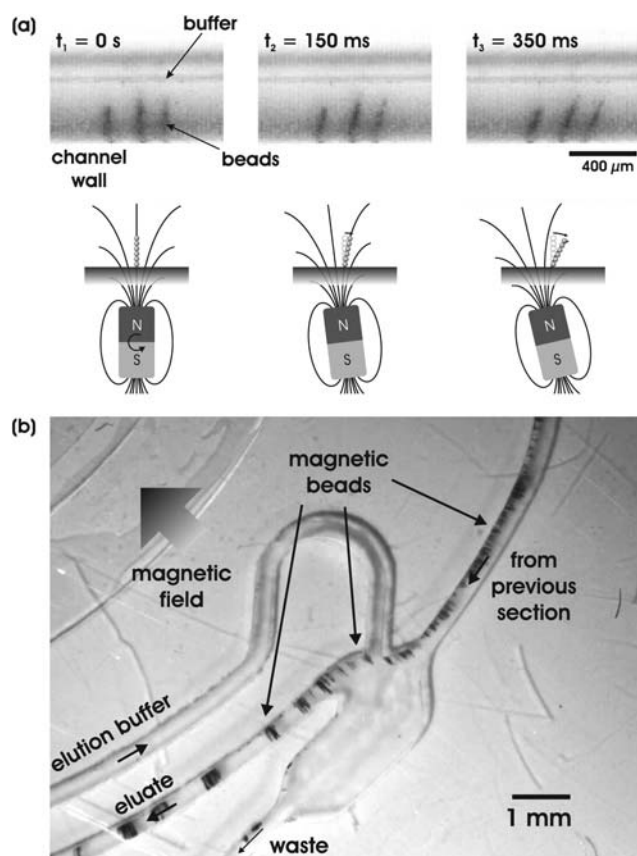


Fig. 3 Illustration of the bead-chain movement. (a) Sequential images of bead chains in a periodically varying magnetic field induced by a rotating permanent magnet ($f = 0.25$ Hz). The magnetic beads align to form flagella-like chains along the magnetic field lines. As the magnetic field rotates, the chains follow the magnetic field lines rotating in the opposite direction (details see text). (b) Snapshot of separation chamber 3. The chains of magnetic beads are strongly attracted by the magnetic field and flow in the vicinity of the inner sidewall throughout the device. The sample inlet flow velocity is 11.9 mm s^{-1} and the average velocity of beads estimated from consecutive images is approximately 0.7 mm s^{-1} . Potentially occurring air bubbles are washed away to the waste through the large outlet of the separation chambers.

At a channel junction two streams of different buffers are brought into contact *via* a laminar-flow interface in order to allow transfer of the magnetic beads from one buffer stream to the other.

In the downstream separation chambers the laminar flow is split into two streams of unequal volume flow rates due to different channel widths of the outlets. Impurities and most of the buffer are continuously washed away to the waste through the larger/wider and outer outlet. The DNA-carrying magnetic beads are transferred to the smaller/narrower and inner outlet. Therefore, the beads are separated from impurities and concentrated in the buffer stream of smaller volume. For effective transfer of the magnetic beads to the smaller/narrower outlet, the flow velocity is reduced by increasing the width of the separation chamber at its entrance.

The channels are arranged in a circular manner around the rotating permanent magnet at the centre. The separation chambers are located as close to each other as possible in order to obtain the shortest transition time from one structure to the next

(see Fig. 2), and thus minimize the transfer time from one buffer to the other. The geometry of the channels between the separation chambers determines the incubation time of the beads in a certain buffer. Hence, processing steps which require longer incubation time can be implemented by simply increasing the channel length.

The rotating permanent magnet is positioned directly underneath the chip, providing sufficient magnetic field for magnetic bead actuation inside the microchannels and the separation chambers. The applied inhomogeneous magnetic field attracts the magnetic beads towards the permanent magnet, resulting in transportation of the beads across the phase interfaces (see Fig. 3b).

Magnetic bead actuation

In order to avoid immobilisation of the magnetic beads on the channel wall, the permanent magnet is continuously rotated using a computer-controlled motor. Thus, the magnetic field shows a periodic variation comprising mainly two phases: a strong magnetic field phase and a weak one.

During the strong magnetic field phase the magnetic beads are attracted effectively towards the inner sidewall of both the separation chambers and the microchannels in between. During this phase, the beads are also transferred across the phase interface of adjacent laminar flows. The beads align with the magnetic field lines, forming flagella-like chains.²² Despite the formation of chains effective buffer exchange at the surface of the beads is still possible.

During the weak magnetic field phase, the bead chains are carried away by the flow, thus preventing the beads sticking on the channel wall as in the case of a static magnetic field.

Materials and methods

Chip production

The two-dimensional layout of the microfluidic structure was designed with CAD software and converted to G-code compatible to a precision milling machine (Minitch Machinery Corporation, Norcross, Georgia 30092, USA). The microchannels were milled directly into a polycarbonate substrate (blank DVD, Sonopress GmbH, Gütersloh, Germany) using a 300 μm milling head (F126.0030, GIS Gienger Industrie-Service, Zurich, Switzerland), with a standard channel depth of 210 μm and width of 300 μm . After the milling process the channels were washed with di-water and isopropanol, dried and sealed with adhesive foil (676070, Greiner Bio-One GmbH, Frickenhausen, Germany). No further surface treatment except the washing was necessary, neither directly after milling nor after the sealing process.

Fluidic actuation

All of the experiments have been performed using buffer solutions provided in a commercially available DNA extraction kit (ajInnuscreen, Berlin, Germany). The different buffers were injected into the chip using glass syringes (1001 TLL, Hamilton, Bonaduz, Switzerland) together with a precision syringe pump (neMESYS, Cetoni, Korbussen, Germany). For defined flow rate settings the syringe pump has been connected to all inlet ports as well as outlet ports leading to the waste. Only outlet port

Table 1 Flow rate configuration for fluidic actuation of the microfluidic chip

Chip port	Flow rate configuration/ $\mu\text{l s}^{-1}$
Inlet 1 (sample)	0.75
Inlet 2	0.75
Inlet 3	1.00
Outlet 1	-0.30
Outlet 2	-0.75
Outlet 3	-1.10
Outlet 4 (eluate)	-0.35

4, from which the DNA eluate is extracted, was not connected to the syringe pump. The eluate was retrieved from one of the two ports of the elution channel (either outlet port 4a was open and outlet port 4b blocked or *vice versa*). The flow rate configuration used in the extraction experiments is listed in Table 1.

Rotation of the permanent magnet

The magnetic beads are manipulated and attracted towards the centre of the chip by a NdBFe permanent magnet (Webercraft, Uster, Switzerland) with a magnetic field strength of 158 mT at a position 3 mm away from the magnet tip. The magnet was mounted on a stepper motor (Nanotec, Landsham, Germany), controlled by a TCM-303 controller (Trinamic, Hamburg, Germany) in combination with an in-house built Visual Basic programme. The rotation speed of the magnet was fixed at 0.25 Hz.

Optical set-up

For optical observation, a high speed camera (pco.1200s b/w, PCO AG, Kelheim, Germany) together with a 12 \times zoom objective (Optometron, Munich, Germany) was used to acquire images and video clips of bead motion inside the chip.

DNA extraction

The on-chip DNA extraction was performed directly from a lysate of *E. coli* (DH5 α Z1).²³ The bacteria were cultured on an agar plate at 37 °C overnight (IPP 500, Memmert, Schwabach, Germany). Then, liquid nutrient medium was inoculated with colonies from the agar plate and incubated on a shaker (POS-300, Grant Instruments Ltd., Shepreth, Great Britain) with 300 rpm at 37 °C overnight. The *E. coli* suspension was then used for DNA extraction.

The lysis buffer of the DNA extraction kit (ajInnucscreen, Berlin, Germany) was used to lyse the bacteria. To ensure reproducible starting conditions 5 ml of the *E. coli* suspension were lysed by incubation with 5 ml lysis buffer at 50 °C for 60 min. Then the lysate was aliquotted and stored at -20 °C for the extraction experiments. The cell count of 1.84×10^9 cfu ml⁻¹ was determined by directly counting the colonies on agar plates using the drop plate method^{24,25} with 30 individual 10 μl drops per dilution step.

For the extraction experiments the lysate was diluted in LB broth and lysis buffer to guarantee the same conditions in each degree of dilution. 250 μl of the sample were mixed with 20 μl of magnetic bead suspension and 250 μl of binding buffer. To

prevent bead agglomeration in the microchannels PEG 8000 (83271, Sigma-Aldrich Chemie GmbH, Munich, Germany) was added to the sample (2% concentration), followed by vortexing of the solution. 450 μl of this sample were then continuously injected into the microfluidic chip to perform the on-chip extraction. During the injection time of 10 min, the beads hardly sedimented, so shaking or stirring was not necessary.

When collecting the eluate at outlet port 4, the magnetic beads still reside within the liquid. To avoid further off-chip elution the beads were removed from the eluate manually directly at the chip outlet.

As a reference an off-chip extraction was performed in test tubes with both the bead-based extraction kit as well as an extraction kit based on spin columns (QiaQuick, Qiagen, Hilden, Germany) according to the instructions of the kit suppliers. As the on-chip extraction yields an eluate volume of 210 μl during a sample collection time of 10 min the same volume of elution buffer has been used in the off-chip experiments to obtain eluates of equal size and to guarantee comparability.

After the on-chip DNA extraction, the ethanol concentration in the eluate was determined using headspace gas chromatography with flame ionisation detection (GC-FID, GC: DANI 86.10 HT, headspace sampler: DANI HSS 86.50).

DNA detection

Directly after the DNA extraction, real-time PCR was carried out to determine the DNA content of the eluate. PCR primer and TaqMan probe have been designed to detect the *Pal* gene of the *E. coli*. The sequences of the primers are:

5'-GGCAATTGCGGCATGTTCTTCC-3' and 5'-TGTTGCATTTGCAGACGAGCCT-3'.

These primers yield a PCR-product with a length of 140 base pairs. The sequence of TaqMan Probe is: 5'^{FAM}-ATGCGAACGGCGGCAACGGCAACATGT-BHQ-1 3'.

The primers and the probe were purchased from Biomers, Germany. Real-time PCR was performed in 10 μl reactions containing 1 μl of template (eluate) on RotorGene 6000 (Corbett Research, Mortlake, Australia) thermocycler according to the following protocol: 95 °C 7 min, (95 °C 15 s and 60 °C 30 s) \times 50.

Results and discussion

Magnetic bead motion

Under the influence of the time-varying magnetic field provided by the permanent magnet, the magnetic beads form flagella-like chains and align along the magnetic field lines. During the strong phase of the magnetic field the beads are attracted to the inner sidewalls of the channel and transferred across the phase interface of the laminar flow. During the weak magnetic field phase the beads are released and transported downstream by the buffer flow.

When the magnet rotates the chains follow the changing orientation of the local magnetic field, thus rolling on the sidewall of the channel. The best results for fast sample turnover were achieved for a rotation of the permanent magnet opposite to the direction of the fluid flow. As illustrated in Fig. 3a the magnetic beads move in the opposite direction compared to the rotation of the permanent magnet. Hence, a rotation against the flow

direction leads to a net bead transport in the flow direction. On the other hand, when the magnet rotates in the same direction as the flow, the varying magnetic field induces upstream-ward bead motion, resulting in a slower bead transport by the counteracting fluid drag.

An inlet flow velocity of 11.9 mm s^{-1} (which corresponds to the flow rate of $0.75 \text{ } \mu\text{l s}^{-1}$) led to an average bead velocity of approximately 0.7 mm s^{-1} , resulting in a sample turnover time of approximately 2 minutes.

Effect of elution channel length

To evaluate the effect of the length of the elution channel (and therefore the incubation time of the magnetic beads within the elution buffer) on the amount of DNA, a comparison of the DNA content of eluates collected from outlet ports 4a and 4b has been made. When the eluate was sampled from outlet port 4a, outlet port 4b was blocked and *vice versa* (Fig. 2).

For this purpose an *E. coli* lysate was prepared and continuously injected into the chip through inlet port 1. After collecting the continuous eluate streams the DNA content within the eluates was determined by qPCR using $1 \text{ } \mu\text{l}$ of eluate per reaction.

In 4 extraction experiments $(8.73 \pm 2.14) \times 10^4$ copies μl^{-1} have been collected from outlet port 4a, whereas 5 extractions collected from outlet port 4b yielded $(1.02 \pm 0.38) \times 10^5$ copies μl^{-1} . This corresponds to an increase in DNA recovery of $\sim 16\%$ when using the longer eluate channel leading to outlet port 4b.

DNA extraction from lysate

The *E. coli* lysate described in the “Materials and methods” section was diluted and mixed with magnetic beads and binding buffer, and then continuously injected into the chip through inlet port 1. The eluate was collected at outlet port 4b as the longer elution channel and therefore longer elution time increases the DNA yield by 16% compared to the shorter elution channel connecting outlet port 4a. Again, for quantification by real-time PCR analysis $1 \text{ } \mu\text{l}$ of the eluate was used. As a reference the DNA was also extracted batch-wise in test tubes. The results are presented in Fig. 4 as well as Table 2.

All three systems show a linear concentration dependency. But at very high DNA concentrations the magnetic beads saturate and hence deviate from this linearity. At very low DNA concentrations (single molecule level) the deviations grow as one copy of DNA more or less has a huge impact on the result.

Nevertheless, the continuous on-chip DNA extraction outperforms the batch-wise bead-based test tube extraction at all dilution factors with relative extraction efficiencies of on average $147 \pm 28\%$.

When compared to the spin column extraction the continuous on-chip DNA extraction achieves an extraction efficiency of approximately $71 \pm 13\%$.

The chromatographic determination of the amount of residual ethanol in 17 eluates from on-chip extractions yielded a concentration of $0.22 \pm 0.10\%$ (v/v), meaning a final concentration of

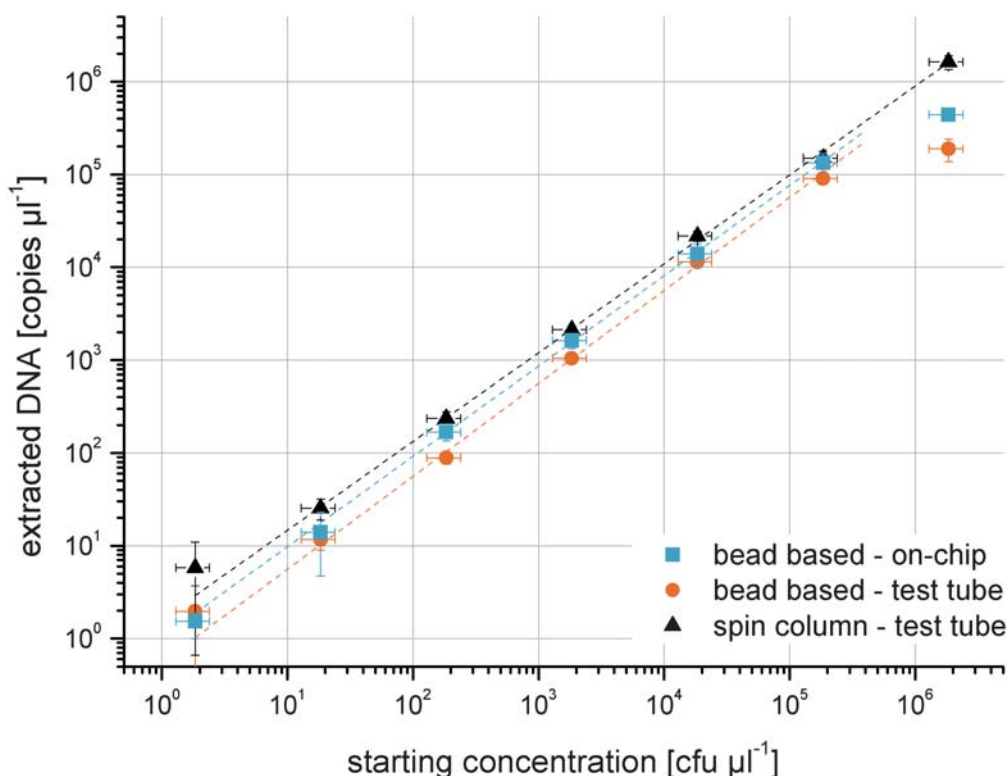


Fig. 4 DNA extraction yield. The amount of DNA extracted was determined by real-time PCR. Shown in the graph is the continuous on-chip extraction as well as the batch-wise reference extractions in spin columns and with magnetic beads. Every data point represents three extraction experiments, which have been analyzed by three real-time PCR reactions each. The standard deviations of the PCR results are depicted as error bars for the amount of extracted DNA. For the starting concentration an error of 30% is assumed. Furthermore, one colony forming unit (cfu) can contain more than a single cell, hence the number of gene copies per cfu can be larger than 1.

Table 2 DNA extraction results. The efficiency ratios have been determined from the mean values of the extraction yields. For calculation of the mean efficiency, the data in brackets have been omitted, as they represent saturation at high concentrations and enormous standard deviations at the single molecule level. As each eluate had a volume of 210 μl the total amount of copies extracted corresponds to the specified concentration multiplied by 210

Starting concentration/cfu μl^{-1}	On-chip bead based/copies μl^{-1}	Off-chip bead based/copies μl^{-1}	Off-chip spin column/copies μl^{-1}	Ratio on-chip/off-chip both bead based (%)	Ratio on-chip/off-chip (spin column) (%)
$(1.84 \pm 0.55) \times 10^6$	$(4.41 \pm 0.38) \times 10^5$	$(1.90 \pm 0.52) \times 10^5$	$(1.63 \pm 0.27) \times 10^6$	(232) ^a	(27.0) ^a
$(1.84 \pm 0.55) \times 10^5$	$(1.34 \pm 0.33) \times 10^5$	$(9.06 \pm 1.23) \times 10^4$	$(1.50 \pm 0.28) \times 10^5$	148	89.5
$(1.84 \pm 0.55) \times 10^4$	$(1.39 \pm 0.37) \times 10^4$	$(1.14 \pm 0.09) \times 10^4$	$(2.17 \pm 0.26) \times 10^4$	122	64.1
$(1.84 \pm 0.55) \times 10^3$	$(1.63 \pm 0.30) \times 10^3$	$(1.05 \pm 0.03) \times 10^3$	$(2.12 \pm 0.20) \times 10^3$	155	76.9
$(1.84 \pm 0.55) \times 10^2$	$(1.68 \pm 0.32) \times 10^2$	$(8.88 \pm 1.28) \times 10^1$	$(2.36 \pm 0.41) \times 10^2$	189	71.1
$(1.84 \pm 0.55) \times 10^1$	$(1.40 \pm 0.93) \times 10^1$	$(1.17 \pm 0.27) \times 10^1$	$(2.55 \pm 0.65) \times 10^1$	120	54.7
$(1.84 \pm 0.55) \times 10^0$	$(1.54 \pm 2.17) \times 10^0$	$(1.96 \pm 1.70) \times 10^0$	$(5.80 \pm 5.14) \times 10^0$	(78.6) ^a	(26.6) ^a
Mean value				147 \pm 28.2	71.3 \pm 13.1

^a Not included in mean value.

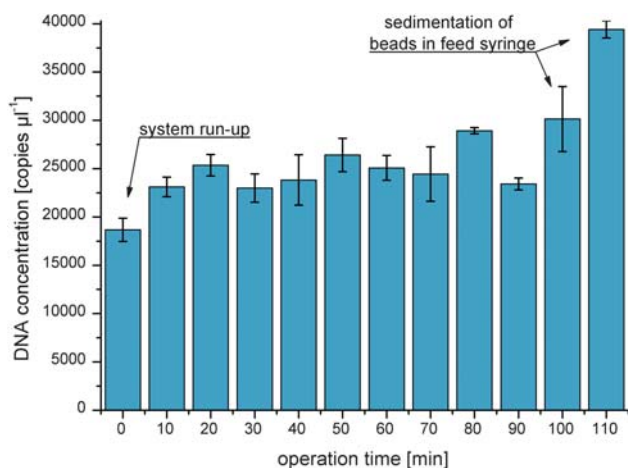


Fig. 5 Continuous long-term on-chip DNA extraction. Lysate with binding buffer and magnetic beads was stored in a syringe. The sample was continuously injected into the microfluidic chip. Starting point ($t = 0$ min) of the measurement was set when the first beads left the chip. The error bars indicate the standard deviation of three real-time PCR analyses. Although the sample in the syringe was mixed every 30 min to avoid sedimentation of the magnetic beads, minimal sedimentation led to a higher bead concentration in the end and therefore a higher DNA concentration in the eluate.

0.02% in the PCR reaction, which is two orders of magnitude below the PCR inhibiting threshold of 2.5% (Rossen *et al.*²⁶ and own data, not shown).

A large sample (5 ml) containing lysate, binding buffer and magnetic beads was prepared to examine the long-term DNA extraction behaviour. The sample was stored in a 5 ml syringe and continuously injected into the chip over a time of 110 min. To avoid or reduce the sedimentation of the magnetic beads the sample was mixed thoroughly every 30 min. Every 10 min a 10 μl sample of the eluate was taken directly from outlet port 4b. The DNA content of the eluate samples was determined by real-time PCR (see Fig. 5).

When the first beads leave the chip the first eluate sample is taken. This indicates the starting point of the measurement ($t = 0$ min). As the beads have just arrived at the outlet port, the bead concentration in the first sample is slightly smaller. Hence, also the DNA content in the first eluate is slightly smaller.

During the course of the experiment the purified amount of DNA remains constant within the error bars. At the end of the experiment slow sedimentation of beads in the feed-syringe takes effect and the bead concentration rises. Accordingly, the DNA content in the eluate increases as well.

Thus the deviation from a constant DNA yield over time results from starting and stopping the experimental procedure. In continuous operation a stable DNA yield per time is obtainable.

In any extraction procedure an enrichment of the target molecule concentration is highly desired. Here, the flow rates in the sample ($0.75 \mu\text{l s}^{-1}$) and elution channels ($0.35 \mu\text{l s}^{-1}$) differ only by a factor of ~ 2 . Therefore, by increasing the ratio a greater concentration could be attained. As some of the injected elution buffer is discarded to the waste through outlet port 3 it forms a diffusion barrier for PCR inhibitors (mainly ethanol) towards the elution channel. Since reducing the eluate flow rate would downsize the diffusion barrier the purity of the eluate would decrease. Hence, increasing the sample flow rate is favourable over reducing the eluate flow rate. This would also offer the possibility to process larger samples in shorter time.

In summary, the continuous DNA extraction on the novel phase-transfer magnetophoresis platform has an extraction efficiency of on average 147% in continuous flow compared to the same extraction system performed batch-wise in a test tube. Residual ethanol concentrations in the eluate are well below the PCR inhibiting threshold.

Conclusions and outlook

In this paper, we introduce a novel platform for continuous DNA extraction and purification based on phase-transfer magnetophoresis using superparamagnetic beads. Utilising a single rotating permanent magnet we apply a very simple and robust method to actuate the beads inside the microfluidic channels.

Based on the novel platform, we demonstrate for the first time a continuous on-chip DNA extraction technique. This technology could complement continuous flow-through PCR which has already been investigated by several groups.^{27–34} The combination of both technologies will enable the implementation of fully integrated systems for continuous nucleic acid based monitoring.

Using appropriate buffer solutions and bead coatings the proposed platform can be used for the continuous automation of

many other analytical assays or preparative protocols, such as immunoassays, cell based assays, as well as the purification of RNA, protein or cells, also including immuno-capture or affinity-precipitation.

Potential applications for continuous monitoring or preparative tasks can be seen in the following fields:

- Epidemiology/Ecology: waste water monitoring of hospitals, e.g. for antibiotic resistant bacteria, such as Methicillin resistant *Staphylococcus aureus* (MRSA)³⁵ or extended-spectrum β -lactamase type bacteria (ESBL).³⁶

- Biodefense: continuous nucleic acid amplification based analysis of air-³⁷ or water-borne³⁸ pathogenic bacteria and viruses.

- Pharma and food industry: (a) bioprocess control³⁹ and (b) continuous monitoring of air borne bacteria in clean rooms.⁴⁰

- Transcriptomics: continuous RNA extraction before and during stimulus for optimisation of array or sequencing based analysis.⁴¹

- Cancer therapy: extracorporeal blood monitoring for feedback controlled drug delivery⁴² during chemotherapy (e.g. monitoring of CEA, carcinoembryonic antigen or drug concentration).

Due to the design on the DVD format the disposable chip is compatible with mass-fabrication in the well established injection compression moulding process used for CD and DVD production.

Future improvements to the continuous DNA extraction procedure reported here will include full integration of continuous on-chip lysis as well as sample enrichment by further reduction of the ratio between eluate- and sample-flow rates.

Acknowledgements

We would like to gratefully acknowledge the consultancy of Dr Thomas Henkel of the Institute of Photonic Technology in Jena, Germany, who recommended suppliers for appropriate pumps and optics, and the guidance of Mr Bernd Faltin of the IMTEK in Freiburg, Germany with the primer design. We also thank Dr Timo Hillebrand, ajInnusec, for providing extraction reagents. The present study is funded by the German Federal Ministry of Education and Research (16SV3528).

References

- 1 D. Mark, S. Haerberle, G. Roth, F. von Stetten and R. Zengerle, *Chem. Soc. Rev.*, 2010, **39**, 1153–1182.
- 2 P. A. Auroux, Y. Koc, A. deMello, A. Manz and P. J. R. Day, *Lab Chip*, 2004, **4**(6), 534–546.
- 3 J. Kim, M. Johnson, P. Hill and B. K. Gale, *Integr. Biol.*, 2009, **1**(10), 574–586.
- 4 J. Wen, L. A. Legendre, J. M. Bienvenue and J. P. Landers, *Anal. Chem.*, 2008, **80**(17), 6472–6479.
- 5 C. W. Price, D. C. Leslie and J. P. Landers, *Lab Chip*, 2009, **9**(17), 2484–2494.
- 6 N. Pamme, *Lab Chip*, 2007, **7**(12), 1644–1659.
- 7 E. P. Furlani, Y. Sahoo, K. C. Ng, J. C. Wortman and T. E. Monk, *Biomed. Microdevices*, 2007, **9**(4), 451–463.
- 8 S. Bronzeau and N. Pamme, *Anal. Chim. Acta*, 2008, **609**(1), 105–112.
- 9 J. Do and C. H. Ahn, *Lab Chip*, 2008, **8**(4), 542–549.
- 10 M. Herrmann, T. Veres and M. Tabrizian, *Lab Chip*, 2006, **6**(4), 555–560.

- 11 M. Herrmann, E. Roy, T. Veres and M. Tabrizian, *Lab Chip*, 2007, **7**(11), 1546–1552.
- 12 J. Pipper, M. Inoue, L. F. P. Ng, P. Neuzil, Y. Zhang and L. Novak, *Nat. Med. (N. Y., NY, U. S.)*, 2007, **13**(10), 1259–1263.
- 13 U. Lehmann, C. Vandevyver, V. K. Parashar and M. A. M. Gijs, *Angew. Chem., Int. Ed.*, 2006, **45**(19), 3062–3067.
- 14 Y. K. Cho, J. G. Lee, J. M. Park, B. S. Lee, Y. Lee and C. Ko, *Lab Chip*, 2007, **7**(5), 565–573.
- 15 R. Hartig, M. Hausmann, J. Schmitt, D. B. J. Herrmann, M. Riedmiller and C. Cremer, *Electrophoresis*, 1992, **13**(9–10), 674–676.
- 16 N. Pamme and A. Manz, *Anal. Chem.*, 2004, **76**(24), 7250–7256.
- 17 P. H. Shih, J. Y. Shiu, P. C. Lin, C. C. Lin, T. Veres and P. Chen, *J. Appl. Phys.*, 2008, **103**(7), 07A316-1–07A316-3.
- 18 C. W. Yung, J. Fiering, A. J. Mueller and D. E. Ingber, *Lab Chip*, 2009, **9**, 1171–1177.
- 19 L. A. Sasso and J. D. Zahn, in Proceedings of the 12th International Conference on Miniaturized Systems for Chemistry and Life Sciences, ed. L. E. Locascio, M. Gaitan, B. M. Paegel, D. J. Ross and W. N. Vreeland, 2008, pp. 77–79.
- 20 S. A. Peyman, A. Iles and N. Pamme, *Lab Chip*, 2009, **9**, 3110–3117.
- 21 M. Karle, J. Miwa, G. Roth, R. Zengerle and F. von Stetten, in Proceedings of the 22nd IEEE International Conference on Micro Electro Mechanical Systems, Ed. C. H. Hierold and P. M. Sarro, 2009, pp. 276–279.
- 22 A. Egatz-Gomez, S. Melle, A. A. Garcia, S. A. Lindsay, M. Marquez, P. Dominguez-Garcia, M. A. Rubio, S. T. Picraux, J. L. Taraci, T. Clement, D. Yang, M. A. Hayes and D. Gust, *Appl. Phys. Lett.*, 2006, **89**(3), 034106-1–034106-2.
- 23 R. Lutz and H. Bujard, *Nucleic Acids Res.*, 1997, **25**(6), 1203–1210.
- 24 H. J. Hoben and P. Somasegaran, *Appl. Environ. Microbiol.*, 1982, **44**(5), 1246–1247.
- 25 B. Herigstad, M. Hamilton and J. Heersink, *J. Microbiol. Methods*, 2001, **44**(2), 121–129.
- 26 L. Rossen, P. Norskov, K. Holmstrom and O. F. Rasmussen, *Int. J. Food Microbiol.*, 1992, **17**(1), 37–45.
- 27 H. Nakano, K. Matsuda, M. Yohda, T. Nagamune, I. Endo and T. Yamane, *Biosci., Biotechnol., Biochem.*, 1994, **58**(2), 349–352.
- 28 A. Reichert, J. Felbel, M. Kielpinski, M. Urban, B. Steinbrecht and T. Henkel, *J. Bionic Eng.*, 2008, **5**, 291–298.
- 29 I. Schneegaß, R. Bräutigam and J. M. Köhler, *Lab Chip*, 2001, **1**, 42–49.
- 30 M. U. Kopp, A. J. de Mello and A. Manz, *Science*, 1998, **280**, 1046–1048.
- 31 M. Hashimoto, P. C. Chen, M. W. Mitchell, D. E. Nikitopoulos, S. A. Soper and M. C. Murphy, *Lab Chip*, 2004, **4**(6), 638–645.
- 32 Y. Y. Li, D. Xing and C. S. Zhang, *Anal. Biochem.*, 2009, **385**(1), 42–49.
- 33 P. J. Obeid, T. K. Christopoulos, H. J. Crabtree and C. J. Backhouse, *Anal. Chem.*, 2003, **75**, 288–295.
- 34 J. Felbel, A. Reichert, M. Kielpinski, M. Urban, N. Hafner, M. Durst, J. M. Kohler, J. Weber and T. Henkel, *Eng. Life Sci.*, 2008, **8**(1), 68–72.
- 35 S. Borjesson, A. Matussek, S. Melin, S. Lofgren and P. E. Lindgren, *J. Appl. Microbiol.*, 2010, **108**(4), 1244–1251.
- 36 D. Li, M. Yang, J. Y. Hu, J. Zhang, R. Y. Liu, X. Gu, Y. Zhang and Z. Y. Wang, *Environ. Microbiol.*, 2009, **11**(6), 1506–1517.
- 37 K. M. Lai, J. Emberlin and I. Colbeck, *Environ. Health Insights*, 2009, **8**, Suppl 1: S15.
- 38 C. J. Woodall, *Desalination*, 2009, **248**(1–3), 616–621.
- 39 M. Diaz, M. Herrero, L. A. Garcia and C. Quiros, *Biochem. Eng. J.*, 2010, **48**(3), 385–407.
- 40 K. Husmann, B. Weidemann and K. J. Steffens, *Pharm. Ind.*, 1999, **61**(2), 170–174.
- 41 M. Beaume, D. Hernandez, P. Francois and J. Schrenzel, *Int. J. Med. Microbiol.*, 2010, **300**(2–3), 88–97.
- 42 D. R. Kryscio and N. A. Peppas, *AIChE J.*, 2009, **55**(6), 1311–1324.